Periodontology 2000, Vol. 67, 2015, 292–311
Printed in Singapore. All rights reserved

The hamster cheek pouch model for field cancerization studies

ANDREA MONTI-HUGHES, ROMINA F. AROMANDO, MIGUEL A. PÉREZ, AMANDA E. SCHWINT & MARIA E. ITOIZ

Oral cancer accounts for 7% of all new cancer cases worldwide, around 270,000 cases annually. In developing countries, it is the fifth most common cancer in men and the seventh most common in women (60, 93, 136). Oral cancer has high morbidity, with a 5-year survival rate of 34–56% (16, 76, 84).

Although the oral cavity is highly visible, most cases of oral cancer are diagnosed at an advanced stage. This is one reason for the poor survival rate (55). An interesting study performed in the province of Córdoba, Argentina, revealed that patients and dentists share equally the responsibility of late diagnosis. Patients delay consultation for an early lesion and dentists fail to identify lesions that warrant referral to a specialist (83).

More than 90% of oral cancers are squamous cell carcinomas, and tobacco use and excessive alcohol consumption, as risk factors, are estimated to account for 75% of all oral cancers in the western hemisphere (48, 135). The particular action of these carcinogens, which exert their effect on the surface of the mucosa, induces the phenomenon known as 'field cancerization'. This concept was introduced by Slaughter et al. (116) to explain the increased risk of malignant transformation in large areas of the epithelial lining of the upper aerodigestive tract. This hypothesis was based on the high incidence of second primary tumors or multifocal cancer, and the concept was later unequivocally supported by the demonstration of molecular changes in the clinically healthy oral mucosa of tumor-bearing patients (10, 125) and in the apparently normal mucosa of smoking patients (10, 12). Furthermore, the sequential or simultaneous development of oral premalignant and malignant lesions in a single patient is the result of progressive genotypic and phenotypic alterations associated with field cancerization (124). Field cancerization has been described in the oral cavity, oropharynx and larynx (10, 24), lung (37), esophagus (100), vulva (104), cervix (21), colon (61), breast (36) and skin (121).

The clinical manifestation of a carcinoma is often preceded by nontumoral lesions of the oral mucosa that are associated with a wide range of clinical and histological features. These lesions have been shown, epidemiologically, to have a higher statistical probability of malignant transformation (73). These clinical entities have been classically termed 'precancerous lesions' and, more recently, have been grouped under the more appropriate term 'potentially malignant disorders' (109, 134). Amongst them, the lesions of greatest prevalence and highest risk of malignant transformation are erythroplasia, leukoplakia, some forms of lichen planus and fibrosis of the submucosa (18, 131).

Histologically, precancerous lesions exhibit epithelial features that can be associated with natural progression to carcinoma (i.e. hyperplasia, slight dysplasia, moderate dysplasia, severe dysplasia and carcinoma *in situ*). The severity of epithelial alterations is directly associated with the risk of malignant transformation. Carcinoma *in situ* is virtually irreversible without appropriate treatment.

It is not yet possible to determine whether a cancerized field will inevitably lead to the development of a carcinoma or whether a dysplastic lesion will progress to malignancy (90). However, the increased risk of development of malignant tumors from a premalignant lesion/condition has been demonstrated epidemiologically.

The search for markers of field cancerization before the appearance of premalignant clinical or histological alterations is relevant in terms of the early diagnosis and prevention of oral cancer (57, 131). Within this context, histochemical markers that can be demonstrated in routine biopsies processed for histopathological diagnosis are of particular significance because detection of a cancerized field may encourage a dentist to perform a closer follow up of those

patients and might constitute an element of persuasion for patients with harmful habits to adopt preventive measures.

The efficacy of early markers of field cancerization must be tested in a model of cancerized mucosa with histological features that resemble those of normal mucosa. Clinically normal areas of the oral mucosa of patients who have already developed tumors have been used as a model of field cancerization to test biomarkers. In a clinical scenario, it is not easy to obtain this type of sample for ethical reasons. Hence, most studies have been performed on surgical specimens, on the histologically normal mucosa adjacent to tumors (39, 43, 69). However, it has been argued that the malignant tumor can result in paracrine effects on the mucosa, inducing metabolic changes that reflect the influence of the tumor rather than the actual status of field cancerization (23).

The use of animal models enables the evaluation of significant amounts of samples, improves reproducibility and avoids the widespread variations known to exist in human entities. Our laboratory has extensively studied the model of chemical cancerization in the hamster cheek pouch in different experimental conditions, including evaluation of histochemical markers of field cancerization.

The hamster cheek pouch model

The model of chemical cancerization in the hamster cheek pouch is the most widely accepted experimental model of oral cancer (20). It was originally developed by Salley, in 1954 (108), and later standardized by Morris, in 1961 (85), to guarantee the reproducibility of the lesions. It is currently the most widely used model for basic biological studies, assessment of therapeutic modalities and chemoprevention (9, 30, 67, 68, 72, 87, 88, 95, 114, 130). The golden hamster, *Mesocricetus auratus*, has an anatomic feature that can be used to advantage (i.e. a pocket within the thickness of the cheek on each side, which only communicates with the oral cavity at the corners of the mouth and is lined with stratified squamous epithelium which resembles that of the oral cavity) (Fig. 1).

The wall of the pouch is separated from the cheek mucosa and the skin by adventitious tissue, a loose connective tissue that allows the pouch to be easily everted (Fig. 2). This is an asset for macroscopic follow up of the tissue response during the experimental period. In addition, certain experimental procedures can be carried out with ease, such as wound induction (94) or local irradiation (111, 113). Furthermore, the pouch is easily accessible *in situ*, allowing for the topical application of chemical carcinogens (Fig. 3).

The model is highly reproducible. It is based on the topical application of subthreshold doses of the complete carcinogen, 7,12-dimethylbenz[a]anthracene. The induced tumors are, in theory, the result of the combined capacities of the carcinogen as an initiator and a promoter. The most widely used protocol involves the topical application of a 0.5% solution of 7,12-dimethylbenz[a]anthracene in mineral oil, three times a week. Exophytic and endophytic tumors begin

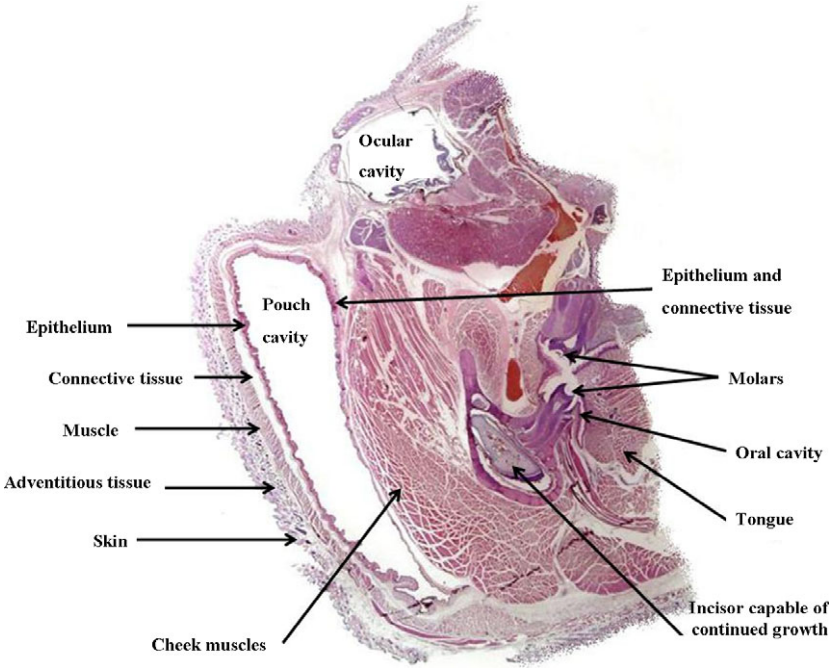

Fig. 1. Localization of the cheek pouch. Microphotograph of a cross-section of a half-head of a hamster. Hematoxylin and eosin stain.

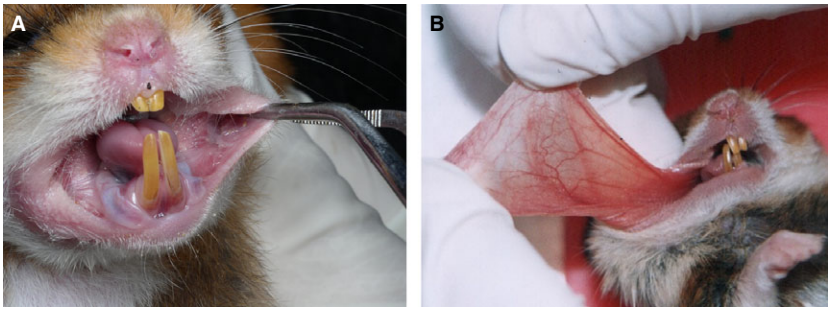

Fig. 2. Access to the hamster cheek pouch (A). Cheek pouch, everted (B).

Fig. 3. Topical application of a carcinogen in the hamster cheek pouch.

Fig. 4. Exophytic carcinoma in the hamster cheek pouch.

to appear at about week 14 (20, 115). Exophytic tumors grow toward the pouch lumen and resemble human oral verrucous carcinomas in terms of hyperkeratinization and growth pattern. However, from the start, these tumors exhibit a large number of cell atypias. Endophytic tumors appear later and infiltrate the thickness of the pouch wall. Histologically, they resemble human squamous cell carcinomas, exhibiting different grades of atypia and differentiation. Exophytic carcinomas are macroscopically the most visible tumors and their growth can be objectively monitored by tumor volume assays in everted pouches. Hence, exophytic tumors are the most widely used tumors in experimental protocols (Fig. 4).

In addition, the model of cancerization in the hamster cheek pouch allows investigation of areas that subsequently develop tumors. These areas have been much less exploited than the tumor tissue in experimental studies. The mode of cancerization in this model, in which the solution of the carcinogen is spread over the whole mucosa, mimics the mode of action of tobacco and alcohol, the two most recognized oral carcinogens (88). However, experimental cancerization is more aggressive than development of human oral cancer because of the concentration and the amount of carcinogen required to guarantee reproducibility of the lesions within the relatively short experimental time-period of the studies. Experimental cancerization induces observable alterations in the oral mucosa within the first week following application of the carcinogen. At that time, a marked desmoplasia is the first change observed underlying the cancerized epithelium, long before abnormal morphologic epithelial lesions occur. The relationship between fibrosis and oral cancer is markedly evident in the occurrence of fibrosis of the submucosa, the well-known precancerous lesion that is highly prevalent in India (96, 97, 119, 120) as a result of the habit of chewing betel. In the hamster model, cancerized oral mucosa with no epithelial alterations constitutes an excellent model of early field cancerization. We have termed this epithelial entity 'no unusual microscopic findings epithelium'.

From the second week of cancerization, premalignant macroscopic and microscopic lesions become evident. The severity of these lesions increases progressively with time. It is possible to establish a

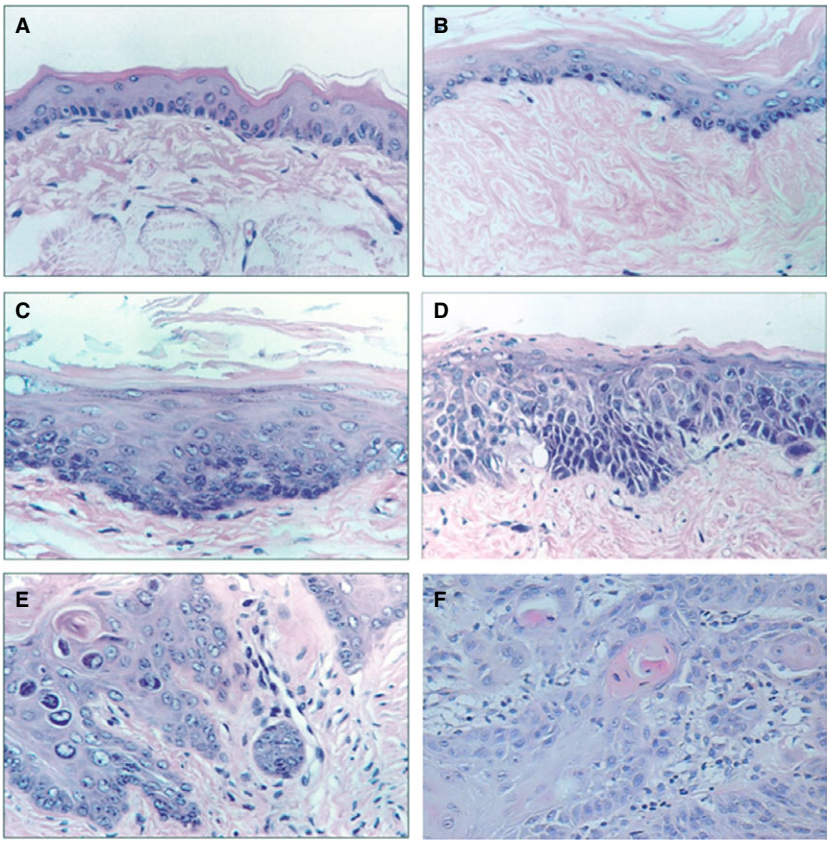

Fig. 5. Progression to carcinoma in the hamster cheek pouch model. (A) Noncancerized, normal epithelium. (B) No unusual microscopic features. (C) Hyperplasia. (D) Severe dysplasia. (E) Microinfiltrating carcinoma. (F) Infiltrating carcinoma. Hematoxylin and eosin stain.

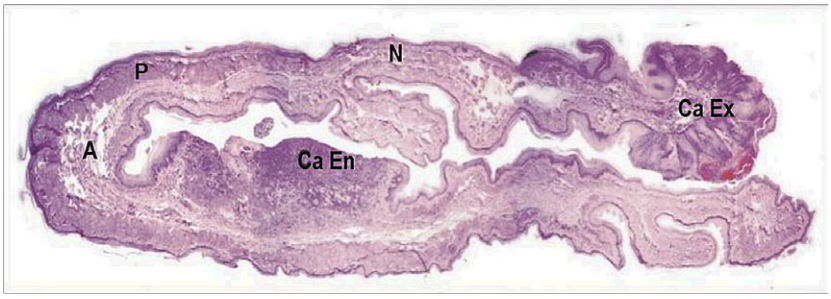

Fig. 6. Panoramic microphotograph of a histological section of a cheek pouch treated topically, for 16 weeks, with the carcinogen 7,12-dimethylbenz[a]anthracene. The pouch was everted and folded in half. When the pouch is everted, the epithelium remains on the surface and the opposite walls are joined by their adventitious tissue (A). The epithelial surface exhibits different stages of the process of carcinogenesis: no unusual microscopic features, with no histological alterations (N), hyperplastic lesions and potentially malignant dysplastic lesions (P), exophytic carcinomas (Ca Ex) and endophytic carcinomas (Ca En).

sequence of lesions, beginning with hyperplasia and hyperkeratosis (very similar to premalignant leukoplakia of the oral mucosa) that predominate in the early stages. These alterations are followed by different degrees of dysplasia, carcinoma *in situ*, microinvasive carcinomas and tumors (Fig. 5). The time point of cancerization and the type of lesion are not strictly correlated (i.e. pouch areas exhibiting different 'lesions' or 'stages' of cancerization can coexist) (Fig. 6). This feature constitutes an additional similarity between the hamster model and spontaneous cancerization in the human oral cavity.

Histochemical markers of field cancerization demonstrable in routine biopsies

Silver staining for nucleolar organizer regions

Nucleolar organizer regions are regions of chromosomal DNA containing genes that code for several ribosomal RNAs. Transcriptionally active nucleolar organizer regions are associated with specific, nonhis-

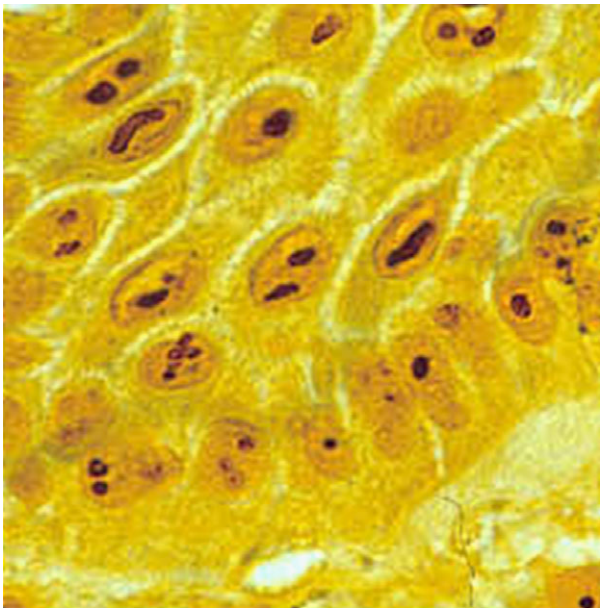

Fig. 7. Nucleolar organizer regions, visualized as intranuclear brown dots of silver precipitate.

tone, acidic, argyrophilic proteins (29, 70, 98) that are selectively identified by a silver colloid staining technique (28) and are visualized as dark brown intranuclear dots at the optical level (Fig. 7). Variations in the normal pattern of silver-stained nucleolar organizer regions indicate qualitative and quantitative changes in protein synthesis (132). An increase in the number of silver-stained nucleolar organizer regions in interphase nuclei indicates hyperactivity, and, in turn, indicates, for different pathological conditions, an increased cell proliferation rate, changes in differentiation processes and secretory activity. These changes usually occur in cells undergoing malignant transformation (27, 28, 58). The silver colloid staining technique can be applied to formalin-fixed, paraffin-embedded tissues and involves a single step of immersion in a solution of gelatin and silver nitrate (56). The simplicity of the staining procedure has led to its widespread application in discriminating between malignant and benign lesions and different degrees of malignancy of some entities in tumor pathology (29, 31, 76, 103). We have reported a sensitive technique (based on the image-analysis evaluation of the parameters of silver-stained nucleolar organizer regions, related to volume and shape) that allows us to detect changes in the silver-stained nucleolar organizer regions which cannot be identified by standard enumeration of silver-stained nucleolar organizer regions. We showed that this method can detect variations in the silver staining of nucleolar organizer regions between different strata of normal epithelium and between human oral papillomas and squamous cell carcinomas (14), and very early cellular alterations, in a model of experimental irradiation of squamous epithelium (112). We then showed the efficacy of the technique to detect changes in the transitional area between normal oral mucosa and squamous cell carcinoma in human biopsies (113). As described above, within certain constraints, this area can be considered a model of early cancerization. Finally, we examined the value of this technique to mark epithelial foci in malignant transformation in the hamster cheek pouch model (111).

7,12-Dimethylbenz[a]anthracene-cancerized pouches and control pouches, which were treated with vehicle (mineral oil) alone, were routinely embedded in paraffin, sectioned and stained by immersion in gelatin–silver nitrate solution. We introduced a rapid pretreatment with nitric acid to reduce background staining and thus improved the accuracy of image analysis (91). Morphometric evaluation of silver-stained nucleolar organizer regions was performed on the following predetermined areas: control epithelium from mineral oil-treated pouches; 7,12-dimethylbenz[a]anthracene-treated epithelium with no unusual microscopic features; epithelia with visible alterations, ranging from hyperplasia to carcinoma *in situ*, which were grouped under the term 'dysplasia'; exophytic tumors; and endophytic carcinomas.

The following morphometric parameters were evaluated: number of silver-stained nucleolar organizer regions per nucleus; the volume of single silver-stained nucleolar organizer regions; the total volume of silver-stained nucleolar organizer regions per nucleus; the proportion of the nuclear volume occupied by silver-stained nucleolar organizer regions; and the shape index of silver-stained nucleolar organizer regions (perimeter/$\sqrt{}$area), which is an expression of shape irregularities (the minimum value of 3.54 corresponds to a perfect circle).

Enumeration of silver-stained nucleolar organizer regions, the parameter classically considered in the literature, revealed the expected statistically significant difference between the control tissue and carcinomas, in keeping with findings in human lesions (27, 56, 70). Changes in the parameters volume and shape reflected an increase in silver-stained material and a tendency for silver-stained nucleolar organizer regions to adopt irregular shapes with the process of carcinogenesis. Interestingly, there were no significant differences in silver-stained nucleolar organizer region counts between control epithelium and epithelium with no unusual microscopic features, but there were significant increases in the single and total volumes of silver-stained nucleolar organizer regions,

Table 1. Number, volume and shape parameters of silver-stained nucleolar organizer regions in different epithelial conditions

Biological parameter	Epithelial condition				
	Control	Cancerized epithelium with no unusual microscopic features	Dysplasia	Exophytic carcinoma	Endophytic carcinoma
Number of silver-stained nucleolar organizer regions	2.26 ± 0.46	1.91 ± 0.39	2.09 ± 0.33	3.49 ± 0.36*	3.80 ± 0.54*
Volume of a single silver-stained nucleolar organizer region	2.04 ± 0.57	3.86 ± 1.11*	2.82 ± 0.71*	2.71 ± 0.92	1.72 ± 0.21
Total volume of silver-stained nucleolar organizer regions per nucleus	4.43 ± 0.84	7.15 ± 1.48*	5.91 ± 1.78*	9.26 ± 2.59*	6.48 ± 0.71*
Total volume of silver-stained nucleolar organizer regions per nucleus/nuclear volume	0.12 ± 0.02	0.15 ± 0.02*	0.13 ± 0.03	0.20 ± 0.03*	0.16 ± 0.02*
Contour index (perimeter/√area)	3.96 ± 0.05	4.11 ± 0.08*	4.01 ± 0.12	4.04 ± 0.09	4.15 ± 0.09*

Values are given as mean ± standard deviation.
*Significant differences with control values ($P < 0.05$).

and alterations in shape were also evidenced (Table 1).

The discriminative value of silver-stained nucleolar organizer region-related parameters in the identification of individual cases of epithelia that fail to exhibit histological alterations (i.e. no unusual microscopic findings) is evident when values from each of the cases are plotted as scattergrams (Fig. 8). These results reveal that morphometric evaluation of silver-stained nucleolar organizer regions is a simple, extremely sensitive technique for detecting incipient cellular alterations of field cancerization that are not evident in routine preparations.

Ploidy analysis

It is widely accepted that accumulation of different genetic alterations is necessary for malignant progression. Among them, mutations affecting normal chromosome segregation may lead to abnormal DNA nuclear content or aneuploidy (41). Cells are generally called aneuploid when their DNA content does not reach the normal diploid value (*2c*) or, much more commonly, when it exceeds the tetraploid value. Most human malignant tumors exhibit different grades of aneuploidy that correlate with histopathology findings and clinical behavior. This knowledge was mainly obtained by applying ploidy analysis with cytophotometric techniques. Quantitative evaluation of nuclear DNA by cytophotometry is less sensitive than molecular cytogenetic or karyotypic analysis and does not provide information on specific chromosomal aberrations. However, as it can be easily performed on fixed histopathology specimens, it has become a useful tool in the diagnosis and prognosis of solid malignant tumors in general and of oral cancer in particular (1, 74, 105, 110, 129). When abnormal amounts of DNA reach certain levels, they can be detected by cytophotometry. This technique has been applied to the study of oral leukoplakia and has shown an association between aneuploidy and histological dysplasia and the risk of malignant transformation (26, 106, 107, 122). The detection of aneuploidy in nondysplastic leukoplakia has been of even greater significance (123), suggesting that aneuploidy is a cause, rather than a consequence, of malignant transformation.

Our studies went on to demonstrate the existence of ploidy alterations in the cancerized field, even before the microscopic manifestation of any morphologic changes, using the hamster cheek pouch model of oral cancer (101). We used Syrian hamsters that were treated with the standard carcinogenesis protocol over a 4-month period, as described above. The control group was composed of hamsters treated with vehicle (mineral oil) alone. Pouches were routinely processed for histopathology. Hematoxylin-and-eosin-stained sections were employed to identify the following histological categories: carcinoma, carcinoma *in situ*, dysplasia, hyperplasia and epithelial areas with no unusual microscopic features. Control areas were

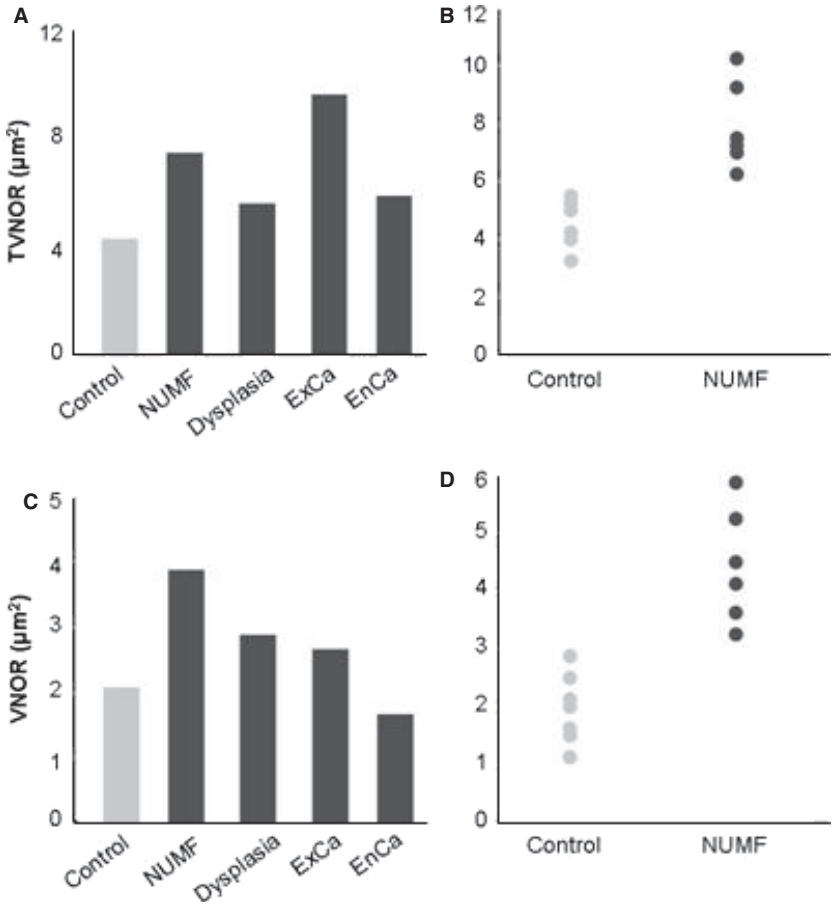

Fig. 8. Bar charts and scattergrams of the total volume of silver-stained nucleolar organizer regions per nucleus (TVNOR) (A, B) and the volume of a single silver-stained nucleolar organizer region (VNOR) (C, D). The scattergrams of control epithelium and cancerized epithelium with no unusual microscopic features (NUMF) show cut-off values of 6 μm^2 for the total volume of silver-stained nucleolar organizer regions per nucleus (B) and 3 μm^2 for the volume of a single silver-stained nucleolar organizer region (D). EnCa, endophytic carcinoma; ExCa, exophytic carcinoma.

taken from cheek pouches treated with vehicle alone. Sections adjacent to hematoxylin-and-eosin-stained sections were processed for Feulgen staining (32). Acid (5N HCl) hydrolysis was performed for 90 min, the time period previously identified on the hydrolysis curve for this material. The areas previously selected on the hematoxylin-and-eosin-stained sections were identified on projections of the Feulgen-stained sections. Ploidy evaluation was performed on each of these areas by employing an image analyzer and DNA measurement software. The DNA content of lymphocytes contained in the section was taken as the diploid (*2c*) reference value. Additional *ad hoc* software was developed by our group to correct errors in measurements resulting from possible differences in section thickness (11, 13). The software calculates the values of total optical density of each nucleus, equivalent to the value of DNA content. In addition, it calculates the mean ploidy value from the mean ratio of total optical density and the total optical density value of the lymphocytes (control *2c* diploid value).

Ploidy histograms (indicating the frequency of occurrence of individual cell ploidy values) were constructed for each histological category. Aneuploidy was objectively computed on the basis of the algorithm defined by Böcking et al. (6, 7) as the *5c* exceeding rate or the aneuploidy index. The *5c* exceeding rate is defined as the percentage of cells with a DNA content of more than *5c*.

Ploidy histograms showed a skew to the right from the diploid value in all the histological categories. The skew increased in relation to the severity of lesions under study. Figure 9 shows an example of characteristic histograms. Interestingly, histologically normal epithelia (regions with no unusual microscopic findings) evidenced a peak with a small deviation within the *2c–4e* region and some events exceeded the tetraploid value.

Mean ploidy and *5c* exceeding rate values are shown in Table 2. As expected, carcinomas and carcinomas *in situ* exhibited a statistically significant increase compared with the control. Mean ploidy values were near the tetraploid range. However, a considerable number of cells exhibited an aneuploid DNA content. The results for preneoplastic areas and histologically normal areas (no unusual microscopic findings) were striking. Mean ploidy was significantly higher than for the control, and aneuploid cells were detected in all of the regions with no unusual microscopic features.

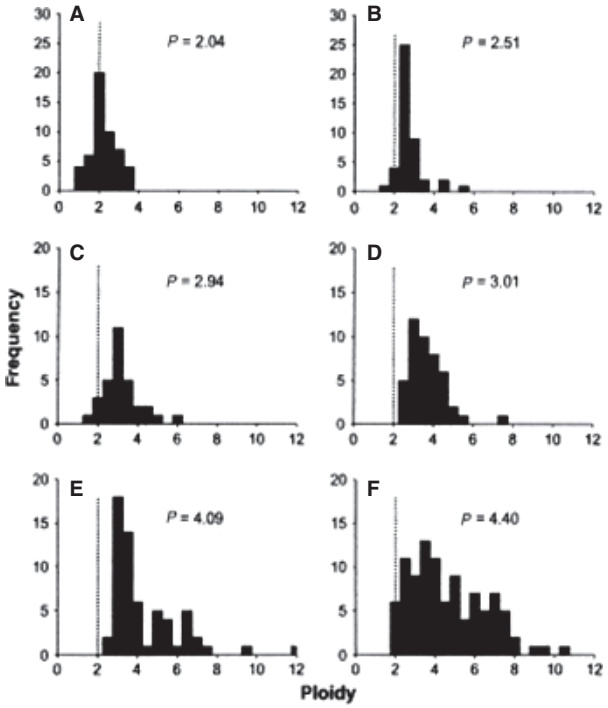

Fig. 9. An example of ploidy histograms for the different histological categories: (A) control epithelium, (B) cancerized epithelium with no unusual microscopic features, (C) hyperplasia, (D) dysplasia, (E) carcinoma *in situ* and (F) carcinoma. Dashed lines indicate the *2c* value. Note the skew to the right and the aneuploid events in the epithelium with no unusual microscopic features.

Table 2. Ploidy analysis in the different stages of carcinogenesis

Histological categories	Ploidy	5c exceeding rate (aneuploidy index)
Control	2.22 ± 0.10	0.33 ± 0.51
Cancerized epithelia with no unusual microscopic features	2.69 ± 0.08[a]	5.70 ± 1.02[a]
Hyperplasia	2.97 ± 0.12[a]	7.14 ± 1.60[a,f]
Dysplasia	2.93 ± 0.15[a]	7.08 ± 1.67[a,f]
Carcinoma *in situ*	2.56 ± 0.33[a]	13.01 ± 3.98[a,b]
Carcinoma	4.35 ± 0.14[a]	12.93 ± 1.92[a,b,c,d,e]

Data are expressed as mean ± standard deviation.
Significance on analysis of variance was followed by *post-hoc* testing using Duncan's test after significant ANOVA ($P = 0.001$): [a], compared with control; [b], compared with cancerized epithelia with no unusual microscopic features; [c], compared with hyperplasia; [d], compared with dysplasia; [e], compared with carcinoma *in situ*; [f], compared with carcinoma.

A *5c* exceeding rate index of 10 (i.e. 10% of cells with a DNA content in excess of 5c) is taken to represent installed malignancy. Percentages ranging between 2% and 4% should be taken to indicate an increased risk of malignant transformation (6, 8, 75, 122). The values of 5.7 ± 1.02 found by us in the no unusual microscopic finding areas of the cheek pouch model reveal that many of these areas exhibit more than five aneuploid events for every 100 epithelial cells.

Most biomarkers that can be used in routine biopsy material, such as those described in this article, can detect changes in biological activity associated with the process of malignant transformation, but are not malignancy-specific markers. Other processes that can give rise to these changes, the most frequent of which is the process of inflammation, must be ruled out when evaluating the risk of malignant transformation. Conversely, the presence of aneuploidy in oral mucosa epithelial cells reveals genetic alterations that are inherent to transformed cells. Ploidy analysis by static cytophotometry on histological sections is a technique that is easy to perform, but requires sophisticated equipment. Provided that access to the equipment is guaranteed, this method is a valuable diagnostic aid in view of the fact that the detection of aneuploid cells is an unequivocal sign of cancerization.

Fibroblast growth factor-2

Epithelium–connective tissue interactions are essential for preserving the structure and function of oral mucosa. Characterization of the changes in the interactions that occur during the development of epithelial neoplasia is important in terms of the basic knowledge of the process and the potential implications of these changes in the control and prevention of malignant transformation (46). Fibrosis and subepithelial vascularization are known to be induced by epithelial factors during tumor development. Using the hamster cheek pouch oral cancer model, we analyzed how early these changes do, in fact, occur. In particular, we focused on the association between these alterations and field cancerization. Within this context, expression of fibroblast growth factor-2 and its receptors, fibroblast growth factor receptor-2 and fibroblast growth factor receptor-3, was assessed by immunohistochemistry at different stages of the carcinogenesis protocol (102).

Fibroblast growth factors are involved in the transmission of signals between the epithelium and connective tissue and influence growth and differentiation of a wide variety of tissues, including epithelia (5). The fibroblast growth factor-2, is one of the prototypes of the large family of growth factors that bind heparin. It is expressed in different tissues and has a wide scope of biologic activities (137). It binds to low-affinity heparin sulfate proteoglycans that are

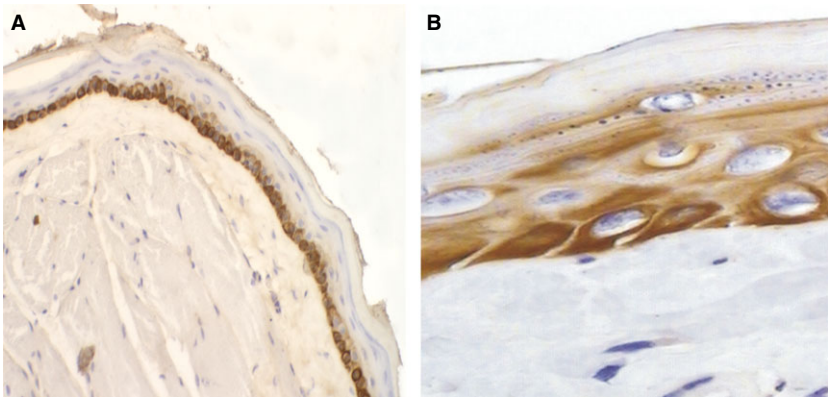

Fig. 10. Immunohistochemical expression of fibroblast growth factor-2. (A) Normal mucosa: the positive reaction is restricted to the basal layer. (B) Epithelium with no unusual microscopic features at 7 weeks of cancerization, showing labeling in all areas of epithelial thickness.

involved in the interaction with high-affinity receptors that, in turn, mediate the cellular response to fibroblast growth factor-2 (25, 66). The fibroblast growth factor receptor family consists of four members that have 55–72% amino acid homology (42).

In the hamster cheek pouch, normal epithelium (without any treatment) expresses fibroblast growth factor-2 in the basal layer. The receptors fibroblast growth factor receptor-2 and fibroblast growth factor receptor-3 are present in all epithelial cells, fibroblasts and endothelia. This finding reveals that, similarly to other tissues, fibroblast growth factor-2 is involved in normal epithelial growth and in the maintenance of connective tissue structures and of the vascular network.

Pouches that had been cancerized for 6–9 weeks exhibited marked increase in the expression of fibroblast growth factor-2. Both the basal cells and the keratinocytes of all the epithelial layers participate in increased synthesis of this factor in areas of epithelium with no unusual microscopic findings, which represents the earliest stage of a cancerized field (discussed in the description of the model given earlier) (Fig. 10).

Seeking to assess this process quantitatively, we calculated the suprabasal labeling index, defined as the number of positive suprabasal cells divided by the total number of suprabasal cells in each selected area. Evaluation was performed using an image analyzer IBAS (Kontron, Jena, Germany). The suprabasal labeling index value peaked at 7 weeks for areas of no unusual microscopic findings, concomitant with the expression of receptors in fibroblasts and endothelia. By this time an intense subepithelial fibrosis had developed (Fig. 11).

Once the epithelial premalignant lesions appear, the number of suprabasal cells expressing fibroblast growth factor-2 continues to rise (Fig. 12). Wakulich et al. (133) reported a similar pattern of behavior in

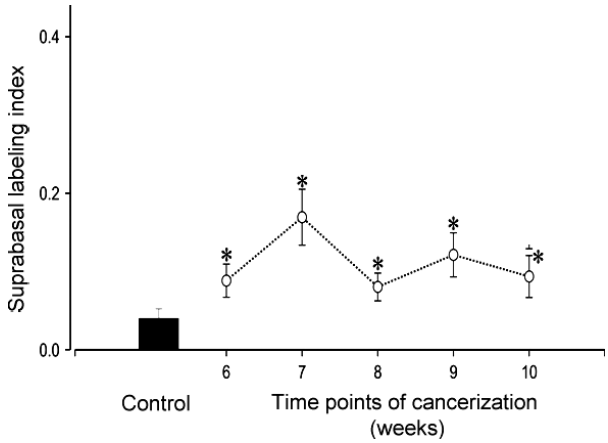

Fig. 11. Quantitative evaluation of the immunohistochemical expression of fibroblast growth factor-2 using the suprabasal labeling index as the end point at intermediate cancerization times (weeks 6–10) for histologically normal epithelia (areas with no unusual microscopic features). *$P < 0.05$ vs. control (*post-hoc* analysis using the Newman–Keuls test).

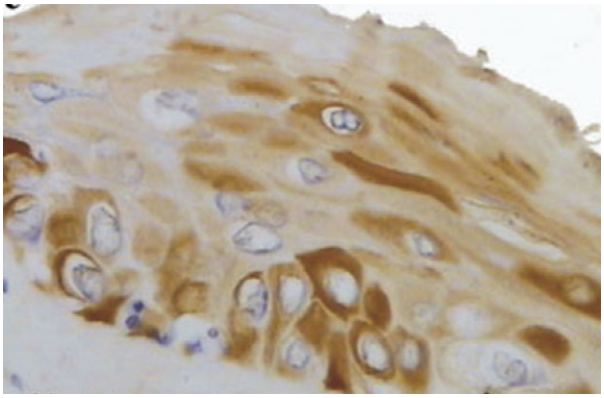

Fig. 12. Immunohistochemical expression of fibroblast growth factor-2 in a dysplastic preneoplastic lesion area. Inhomogeneous expression in basal and suprabasal layers.

human oral dysplasia. Most of the carcinomas fail to express fibroblast growth factor-2, and, when they do, the labeling is faint and heterogeneous. These varia-

tions in labeling are in keeping with the data reported by Janot et al. (59) for human carcinomas.

Taken as a whole, the behavior of fibroblast growth factor-2 in the cheek pouch model is in agreement with the data reported on its expression in carcinomas and potentially malignant lesions of the human oral mucosa. In addition, we found that the increase in fibroblast growth factor-2 activity is most marked during the early stages of epithelial malignant transformation, before there is evidence of clinical or histological alterations.

Epithelial proliferation

Epithelial basal cells of the oral mucosa proliferate by mitosis. Each cell that enters the cell cycle gives rise to two cells that inherit the genetic material from the progenitor cell. Entry into the cell cycle is strictly controlled by signaling, resulting from the interaction with neighboring cells. This interaction occurs in normal conditions (e.g. for replacement of desquamating cells) or in pathological conditions, such as inflammation or wound healing. Malignant cells, transformed by genetic mutations, are able to replicate, regardless of control mechanisms. Even cells with early genetic alterations (initiated cells) can escape the normal control mechanisms of the cell cycle. When these mutated cells continue to proliferate, new mutations arise that confer progressively more growth benefits on the tissue and lead to the development of a malignant tumor.

Cancerization of the hamster cheek pouch provides an excellent model for studying the variations in proliferation in morphologically normal, cancerized tissue areas. These areas that we have called no unusual microscopic findings (see description of the model above) are lined by an epithelium with no histological alterations that, in turn, lines a desmoplastic connective tissue with no congestion or inflammatory infiltrate. Hence, during this period, the action of substances, in the microenvironment, that induce proliferation is minimal.

One technique that is easy to apply to the study of proliferation in experimental material is the counting of cells labeled immunohistochemically following the incorporation of 5-bromo-2′-deoxyuridine. The technique is based on the incorporation of this nucleoside (a structural analogue of thymidine) by cell DNA during the phase of synthesis needed for duplication. 5-Bromo-2′-deoxyuridine is injected into the animal 30 min before it is killed. During this time, the compound is incorporated by the cells that are synthesizing DNA. The availability of 5-bromo-2′-deoxyuridine exceeds, by far, the availability of constitutive thymidine. Following death of the animal, and sampling and histological processing of the material, the cells that have incorporated 5-bromo-2′-deoxyuridine into their genetic material can be labeled using a specific anti-(5-bromo-2′-deoxyuridine) serum (Fig. 13).

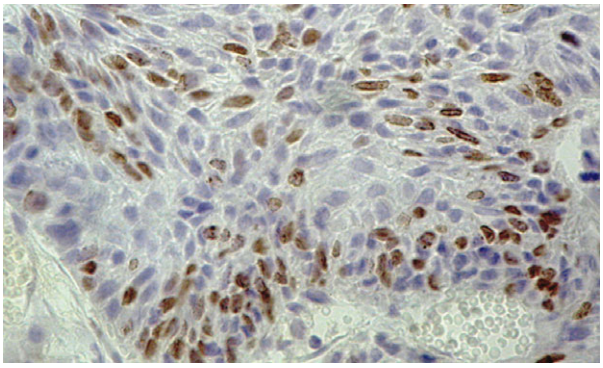

Fig. 13. Immunolabeling of nuclei synthesizing DNA: uptake and subsequent immunohistochemical demonstration of 5-bromo-2′-deoxyuridine. Background staining with hematoxylin shows the nuclei of quiescent cells in blue.

As part of a more extensive study of the effects of boron neutron capture therapy on field cancerized tissue (discussed later; 50) we studied the proliferative activity of normal and potentially malignant tissue of the hamster cheek pouch. 5-Bromo-2′-deoxyuridine-labeled cells were counted by light microscopy at 400× magnification as marked nuclei above a fixed length (300 μm) of basal layer, employing a grid fitted into the eyepiece.

The number of epithelial cells synthesizing DNA increases significantly in cancerized epithelium before the appearance of histological changes (Fig. 14) and increases progressively with the progressive development of epithelial alterations (Table 3).

An increase in the counts of labeled cells in apparently normal oral mucosa without signs of inflammation suggest the existence of transformed cells with the ability to undergo uncontrolled proliferation. This finding is in keeping with the demonstration of aneuploid cells in these tissues (discussed earlier in the section on ploidy studies).

These data can be extrapolated to a clinical scenario as an additional tool to identify field cancerized tissue. Obviously, 5-bromo-2′-deoxyuridine labeling cannot be used in human biopsies because the technique requires prior injection of large amounts of the nucleoside. However, this technique can be replaced by labeling with endogenous markers related to the cell cycle, such as nuclear antigens (Ki-67) or nuclear proteins associated with polymerases (e.g. proliferating cell nuclear antigen).

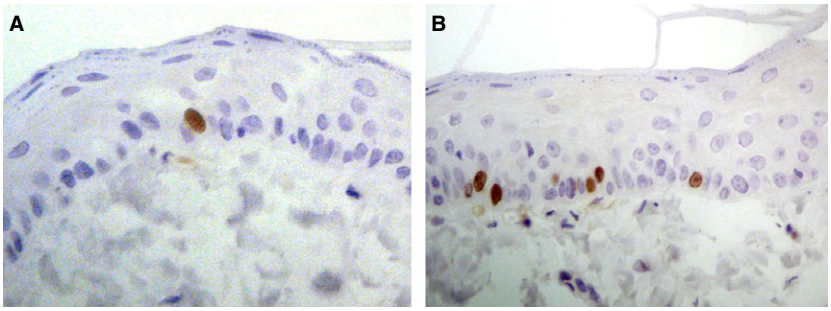

Fig. 14. Proliferating nuclei in untreated epithelium (A) and in epithelium with no histological changes (i.e. areas with no unusual microscopic features) at 7 weeks of cancerization (B). The areas with no unusual microscopic features exhibited an increase in nuclei synthesizing DNA. Proliferating nuclei were labeled immunohistochemically with anti-(5-bromo-2′-deoxyuridine) serum.

Table 3. Number of 5-bromo-2′-deoxyuridine-labeled nuclei/field for normal cheek pouch epithelium and after 14 weeks of cancerization with 7,12-dimethylbenz[a]anthracene

Tissue type	Number of 5-bromo-2′-deoxyuridine-labeled nuclei/field (mean ± standard deviation)	Total number of fields measured
Normal epithelium	0.81 ± 1.22	758
Potentially malignant tissue		
Cancerized epithelia with no unusual microscopic findings	4.0 ± 3.6*	618
Hyperplasia	9.2 ± 6.9*	286
Dysplasia	18.0 ± 9.5*	79

*Statistically significant difference vs. the normal value ($P < 0.001$).

Indicators of angiogenesis

Preneoplastic cells release pro-angiogenic mediators. We currently know that angiogenesis precedes tumor development (33, 34, 44), in which pretumoral tissue induces the formation of blood vessels for its own supply and the subsequent nutrition of tumor tissue.

The time at which the quiescent tumor vasculature is activated to produce new capillaries has been termed the angiogenic switch (4, 17, 47). The angiogenic switch depends on the balance between pro- and anti-angiogenic signals and can occur in different pretumoral stages for different neoplasms. The signals that trigger the angiogenic switch include metabolic stress induced by hypoxia, genetic mutations that activate oncogenes or inactivate tumor suppressor genes (3) and, mainly, the rise in mediators such as fibroblast growth factor and, more importantly, vascular endothelial growth factor, a major pro-angiogenic factor well documented to induce vascular endothelial cell proliferation and vascular sprouting.

Seeking to assess variations in angiogenesis in pretumoral stages of the hamster cheek pouch oral cancerization model and to determine the angiogenic switch, we evaluated vascular endothelial growth factor activity, endothelial cell proliferation, vascular density and changes in vascular morphology in epithelia with potentially malignant lesions.

The variations in the levels of the pro-angiogenic factor, vascular endothelial growth factor, were evaluated by immunohistochemical labeling with anti-human vascular endothelial growth factor serum (Santa Cruz Biotechnology, Dallas, TX, USA) and scoring of the intensity of the reaction from 0 to 2, as follows: 0, negative, or less intense than a standardized kidney control mounted on each slide; 1, moderate, or equal to the control; 2, intense, or stronger than the control. Analysis of the proliferation rate of endothelial cells was performed by intraperitoneal injection and subsequent detection of 5-bromo-2′-deoxyuridine, using the method described earlier, in the section entitled ‘Epithelial proliferation’. Analyses of vascular density and of changes in the shape of vascular sections were performed by immunolabeling vascular walls using anti-FVIII serum (126) and by evaluation of vascular sections. The evaluation of vascular morphology involved image analysis, using appropriate software, of digital images of immunolabeled

vascular sections (45, 92). The end-points area, perimeter and circularity were evaluated for each vascular section. According to Padera et al. (92), the parameter, circularity, is considered to be an indicator of vascular compression. A value of circularity of 1.0 corresponds to a perfect circle, hypothetically representative of a normal blood vessel, free from compressive forces and with optimal perfusion. The circularity value progressively nears 0.0 as the shape of the vascular section becomes an elongated polygon owing to an increase in the difference between diameters. This change would indicate that the blood vessel is undergoing greater compression and concomitant alterations in perfusion.

The results show that expression of vascular endothelial growth factor in the normal cheek pouch epithelium is very low or absent altogether (score 0). Expression of vascular endothelial growth factor is higher in cancerized epithelium in areas of no unusual microscopic features and in areas of hyperplasia and dysplasia (potentially malignant lesions) all of which score between 1 and 2, with no differences in the staining between the three areas (Fig. 15). The influence of pro-angiogenic factors secreted by the epithelium is evident histologically in the underlying connective tissue when dysplastic lesions have already developed. Uptake of 5-bromo-2′-deoxyuridine by endothelial cells indicates their proliferative status. The 5-bromo-2′-deoxyuridine-positive cell count was 5.46 + 9.67 per mm^2 (number of animals = 11), whereas, in normal cheek pouch, epithelial capillary proliferation is virtually absent (i.e. 5-bromo-2′-deoxyuridine-positive cell count = 0). Vascular density decreases in areas of no unusual microscopic findings, probably because of the presence of fibrosis. Conversely, it increases significantly in areas lined by hyperplastic and dysplastic epithelium (Table 4, Fig. 16). Furthermore, in these areas, the blood vessels are dilated and exhibit changes in shape (Fig. 17), indicating that vascular compression begins in the early stages of malignant transformation.

Table 4. Number of blood vessels/mm^2 of subepithelial connective tissue underlying different tissue areas

Tissue area	Number of blood vessels/mm^2 (mean ± standard deviation)
Normal epithelium	85.08 ± 48.32
Cancerized epithelia with no unusual microscopic findings	58.08 ± 25.00
Hyperplasia	108.63 ± 96.11
Dysplasia	182.63 ± 104.80***
Tumor	68.43 ± 64.43

***$P < 0.05$ (dysplasia vs. normal epithelium).

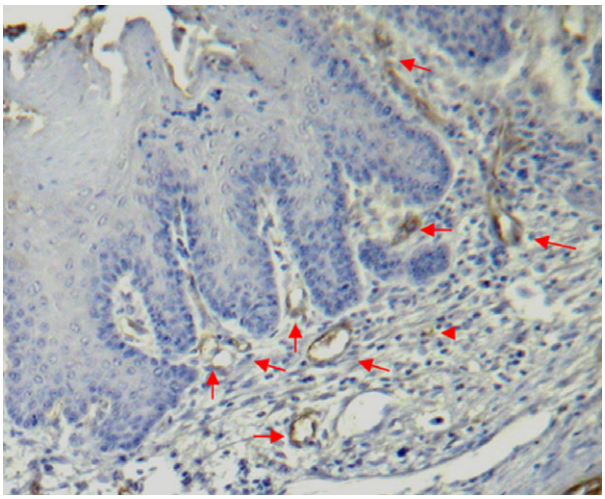

Fig. 16. Angiogenic switch in the connective tissue underlying dysplastic epithelium. The arrows indicate numerous capillaries immunostained with anti-FVIII Ig.

The hamster cheek pouch model for boron neutron capture therapy studies: response of field cancerized tissue

As previously described, the hamster cheek pouch oral cancer model poses a unique advantage in that the carcinogenesis protocol mimics the spontaneous process of malignant transformation, leading to the development of tissue with potentially malignant

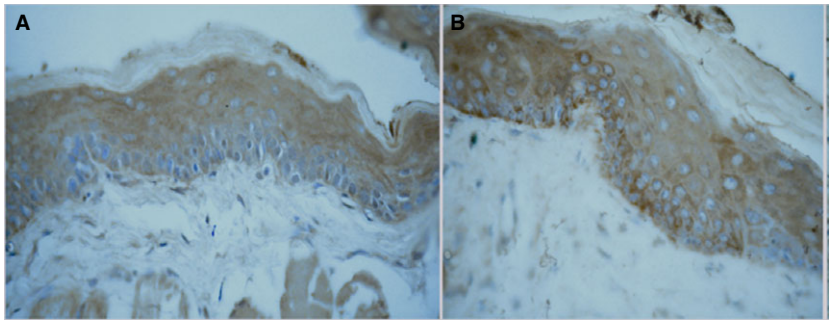

Fig. 15. Expression of vascular endothelial growth factor. (A) Normal oral mucosa. (B) Potentially malignant epithelium: a stronger immunolabeling reaction is observed in this tissue.

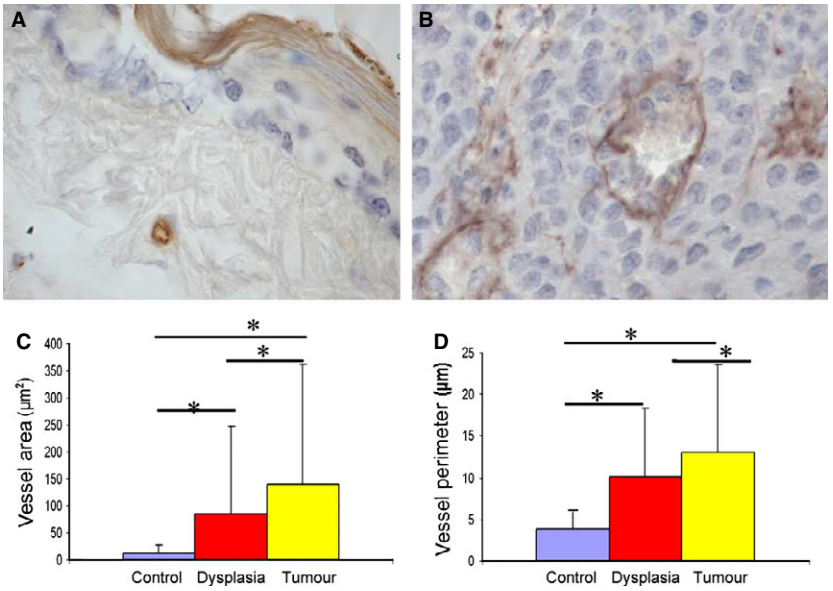

Fig. 17. Vascular changes. (A) Area underlying normal epithelium. (B) Area underlying dysplastic epithelium. There was a progressive increase in vessel area (C) and perimeter (D) in areas underlying dysplastic epithelium and in tumor stroma compared with vessels in control pouches. Each bar indicates the mean value with standard deviation. $*P < 0.05$.

disorders from which tumors arise (50). Thus, the model allows for the study of both tumors and field-cancerized tissue (10, 89), unlike implanted tumor models. In addition, it is an accepted model of mucositis and enables assessment of the side effects of radiotherapy and chemotherapy (9).

The relevance of field cancerization in head and neck cancer lies in the frequent occurrence of second primary tumors after treatment (40). There is a risk of approximately 20% for second primary tumors based on continued exposure to risk factors (54). In addition, in head and neck cancer, the incidence of recurrent disease may be as high as 30–50% after radiotherapy (e.g. 35). Within this context, recurrent and/or second primary tumors are a therapeutic challenge in head and neck cancer. In addition, the constraints imposed on therapeutic protocols by the dose-limiting nature of tissue with potentially malignant disorders must be assessed. In a clinical scenario, confluent oral mucositis is a frequent, dose-limiting side effect during conventional radiotherapy for advanced head and neck tumors (117, 118), affecting approximately 80% of patients (118).

Given the relatively poor overall 5-year survival rate for malignancies of the oral cavity (76), and in view of the fact that radical surgery causes large tissue defects (64), there is a need for more effective and selective therapies. Within this context, boron neutron capture therapy has been proposed for the treatment of head and neck cancer (e.g. 62, 63). Boron neutron capture therapy is a binary treatment that combines the administration of boron carriers (which are taken up preferentially by neoplastic tissue) with irradiation with a thermal/epithermal neutron beam. The high linear energy transfer α-particles and recoiling ^{7}Li nuclei emitted during the capture of a thermal neutron by a ^{10}B nucleus have a high relative biological effectiveness (e.g. 22, 38). Their short range (6–10 μm) in tissue limits the damage largely to cells containing ^{10}B. In this way, boron neutron capture therapy targets neoplastic tissue selectively, sparing normal tissue. However, the interaction of the neutrons with nitrogen and hydrogen in tissue, and the gamma component of the beam, will deliver an unavoidable and nonspecific background dose (22, 128). Boron neutron capture therapy protocols are designed to maximize the boron component of the dose and to minimize background dose. As boron neutron capture therapy is based on biological, rather than geometric, targeting, it would be suited to treat undetectable micrometastases (15) and foci of malignant transformation in field-cancerized tissue (80, 81).

The hamster cheek pouch model of oral cancer was proposed and validated by our group for boron neutron capture therapy studies to explore new applications of boron neutron capture therapy, study its radiobiology and improve its therapeutic efficacy (67, 68). Our first experimental studies preceded the first clinical trial of boron neutron capture therapy for head and neck malignancies (65). We evidenced the therapeutic efficacy of boron neutron capture therapy, mediated by the boron compounds boronophenylalanine and/or decahydrodecaborate, to treat oral cancer in this experimental model with no normal tissue radiotoxicity, and slight/moderate mucositis in dose-limiting tissue with potentially malignant disorders surrounding tumors (2, 49, 50, 53, 67, 68, 77,

78, 79, 99, 127, 128). Despite the success of the boron neutron capture therapy protocols employed in these studies to treat tumors, the inhibition of tumor development in tissue with potentially malignant disorders remains an unresolved challenge. We showed that boron neutron capture therapy induces a drastic fall of DNA synthesis in tissue with potentially malignant disorders, associated with a short-term lag in the development of recurrent and/or second primary tumors (50). However, the aggressiveness of the model, as employed in tumor control studies (e.g. 67, 99, 78, 127, 128), precludes the long-term follow-up (19) needed to evaluate the effect of boron neutron capture therapy on tissue with potentially malignant disorders in terms of the development of recurrent and/or secondary primary tumors. Therefore, we developed a model of oral precancer in the hamster cheek pouch that can be used for long-term studies (i.e. is amenable to long-term (8 months) follow-up, but, if left untreated, guarantees tumor development in ≥90% of the animals) (52). Being less aggressive, it mimics human oral carcinogenesis more closely than the standard carcinogenesis protocol (86). This carcinogenesis protocol involves the topical application of 7,12-dimethylbenz[a]anthracene, twice a week, for 6 weeks. Long-term follow-up is favored as it reduces the number of applications of 7,12-dimethylbenz[a] anthracene, which is known to cause liver disorders, such as enhanced oxidation of lipids and proteins, and, coupled with compromised antioxidant defenses (71) contributes to the decline of test animals.

Employing this model of oral precancer for long-term follow-up, we first performed boron biodistribution studies employing different administration protocols of boron compounds and showed the therapeutic potential of these administration protocols (80). Boron biodistribution studies are performed to determine the concentration of boron in tissue and blood, on which the dose calculations are based, and to select the optimal time point, postadministration, for performing neutron irradiation. This time point is selected to maximize the ratio of boron concentration between target and normal tissue and target tissue and blood (e.g. 51). We then demonstrated the partial inhibitory effect vs. control (cancerized, untreated pouches) on the development of tumors in tissue with potentially malignant disorders of a single application of boron neutron capture therapy mediated by the boron compounds borono-phenylalanine (SBPA-BNCT), decahydrodecaborate (SGB-10-BNCT) or decahydrodecaborate + borono-phenylalanine (S(GB-10+BPA)-BNCT) at 4 Gy absorbed dose, prescribed for tissue with potentially malignant disorders, with no normal tissue radiotoxicity and without severe dose-limiting mucositis in tissue with potentially malignant disorders (80). All three boron neutron capture therapy protocols induced a statistically significant reduction in tumor development in tissue with potentially malignant disorders, reaching a maximal inhibition of 77–100%. The inhibitory effect of borono-phenylalanine–boron neutron capture therapy and decahydrodecaborate + borono-phenylalanine–boron neutron capture therapy persisted at 51% at the end of follow up (8 months), whereas the inhibitory effect of decahydrodecaborate–boron neutron capture therapy showed a marked decrease after 2 months (Fig. 18). At 8 months post-treatment with borono-phenylalanine-boron neutron capture therapy and decahydrodecaborate + borono-phenylalanine-boron neutron capture therapy, the tissue with potentially malignant disorders that did not give rise to tumor development had regained the macroscopic and histological appearance of normal (noncancerized) pouches (Fig. 19). We then demonstrated that a double application, 6 weeks apart, of borono-phenylalanine-boron neutron capture therapy and deca-

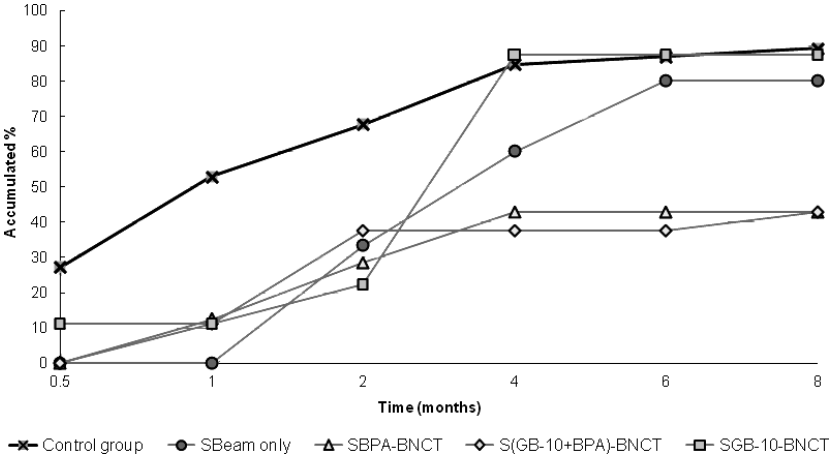

Fig. 18. Accumulated percentage of animals that develop 'new' tumors from tissue with potentially malignant disorders at representative time points post-treatment. S(GB-10 + BPA)-BNCT, Single application of Boron Neutron Capture Therapy (BNCT) mediated by the boron compounds GB-10 and BPA; SBeam only, Single application of Beam only; SBPA-BNCT, Single application of BNCT mediated by the boron compound BPA; SGB-10-BNCT, Single application of BNCT mediated by the boron compound GB-10.

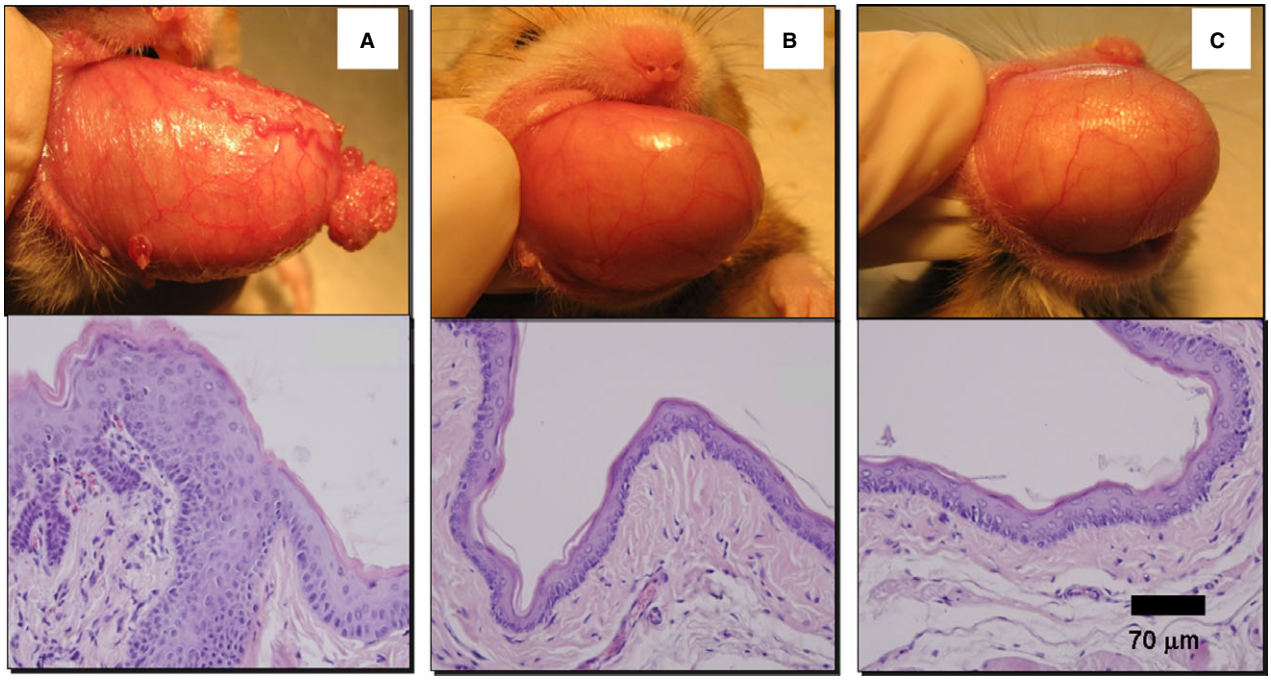

Fig. 19. Representative macroscopic views of: (A) control (cancerized, not treated) field-cancerized pouch with tumors; (B) a field-cancerized pouch treated with Single application of boron neutron capture therapy mediated by the boron compound BPA (SBPA-BNCT) that had not developed tumors 8 months post-treatment; and (C) a normal pouch (noncancerized). Below the macroscopic views we show, for each case, the corresponding characteristic light microscopy images (hematoxylin and eosin stain). Note that the field-cancerized pouch treated with SBPA-BNCT has the macroscopic and histological appearances of a normal (noncancerized, not treated) pouch.

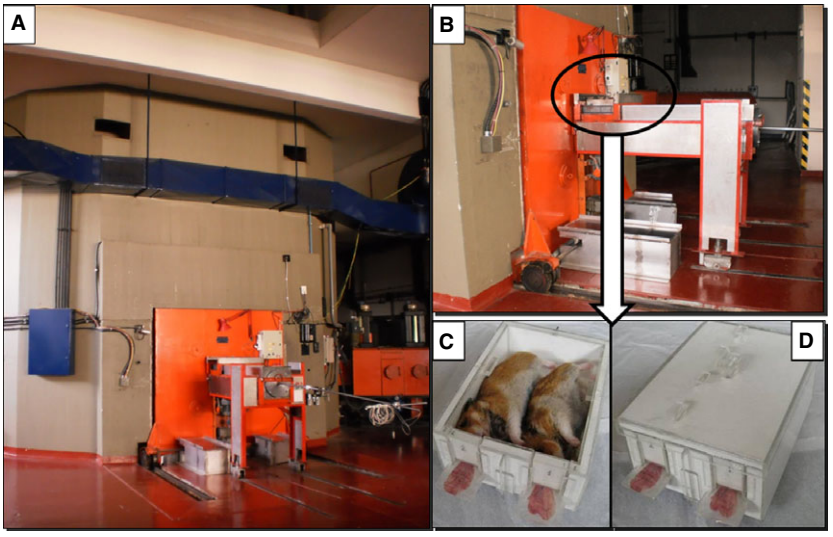

Fig. 20. (A) External view of the RA-3 nuclear reactor thermal neutron facility. (B) External view of the space for sample insertion (circle). The samples are then moved to the irradiation position near the reactor core. (C) Animals ready for irradiation: lithium-6 carbonate shielding is used to protect the body of the animal (the enclosure is shown without its lid). The cheek pouch is everted out of the enclosure onto a protruding shelf for exposure. (D) Lithium-6 carbonate shielding to protect the body of the animal (the enclosure is shown with its lid).

hydrodecaborate + borono-phenylalanine-boron neutron capture therapy, at 8 Gy total absorbed dose, could be used therapeutically, at no additional cost in terms of radiotoxicity, in normal tissue and in the tissue with potentially malignant disorders (80). The animals were irradiated at the RA-3 thermal facility, employing a lithium-6 carbonate shield to protect the body of the animal with the cheek pouch everted out of the enclosure onto a protruding shelf for exposure (99) (Fig. 20). The mean thermal neutron flux at the center of the shelf was $7.49 \times 10^9 \pm 1.6 \times 10^9$ n/cm^2.s and the mean gamma dose rate at the irradiation position was 6.08 ± 0.61 Gy/h.

Seeking to optimize boron neutron capture therapy in terms of improving therapeutic efficacy and reducing radiotoxicity, we evaluated new boron neutron capture therapy protocols, in which tumor development was inhibited and radiotoxicity minimized, in

the hamster cheek pouch model of oral precancer for long-term studies. We showed that a double application (4 weeks apart) of decahydrodecaborate + borono-phenylalanine-boron neutron capture therapy, at a total dose of 10 Gy, rendered the best therapeutic advantage (i.e. 63–100% inhibition of tumor development with only slight mucositis in 67% of cases) (82).

Issues such as dose levels and dose fractionation, interval between applications and choice of boron compounds are pivotal in conveying the optimal therapeutic advantage and must be tailored for a particular pathology and anatomic site. Within this context, the hamster cheek pouch model of oral cancer and precancer for long-term studies can be employed in radiobiological boron neutron capture therapy studies to determine treatment conditions that would provide an optimal protocol of boron neutron capture therapy and that would warrant cautious assessment in a clinical scenario.

References

1. Abou-Rebyeh H, Burgmann V, Nagel R, Al-Abadi H. DNA ploidy is a valuable predictor for prognosis of patients with resected renal cell carcinoma. *Cancer* 2001: **92**: 2280–2285.
2. Aromando RF, Trivillin VA, Heber EM, Pozzi E, Schwint AE, Itoiz ME. Early effect of boron neutron capture therapy mediated by boronophenylalanine (BPA–BNCT) on mast cells in premalignant tissue and tumors of the hamster cheek pouch. *Oral Oncol* 2010: **46**: 355–359.
3. Bergers G, Hanahan D, Coussens LM. Angiogenesis and apoptosis are cellular of neoplastic progression in transgenic mouse models of tumorigenesis. *Int J Dev Biol* 1998: **42**: 995–1002.
4. Bergers G, Benjamin LE. Tumorigenesis and the angiogenic switch. *Nat Rev Cancer* 2003: **3**: 401–410.
5. Bikfalvi A, Klein S, Pintucci G, Rifkin DB. Biological roles of fibroblast growth factor-2. *Endocr Rev* 1997: **18**: 26–45.
6. Böcking A, Adler CP, Common HH, Hilgarth M, Granzen B, Auffermann W. Algorithm for a DNA-cytophotometric diagnosis and grading of malignancy. *Anal Quant Cytol* 1984: **6**: 1–7.
7. Böcking A, Schunk K, Auffermann W. Exfoliative-cytologic diagnosis of basal cell carcinoma, with the use of DNA image cytometry as a diagnostic aid. *Acta Cytol (Baltimore)* 1987: **31**: 143–149.
8. Böcking A. DNA cytometric diagnosis of prospective malignancy in borderline lesions of the uterine cervix. *Recent Results Cancer Res* 1991: **122**: 106–115.
9. Bowen JM, Gibson RJ, Keefe DMK. Animal models of mucositis: implications for therapy. *J Support Oncol* 2011: **9**: 161–168.
10. Braakhuis BJM, Tabor MP, Kummer JA, Leemans CR, Brakenhoff RH. A genetic explanation of Slaughter's concept of field cancerization. *Cancer Res* 2003: **63**: 1727–1730.
11. Brandizzi D, Itoiz ME, Lanfranchi HE, Keszler A, Cabrini RL. Use of correction procedures in ploidy analysis of oral carcinomas. *Acta Odontol Latinoam* 2002: **15**: 39–44.
12. Brennan JA, Boyle JO, Koch WM, Goodman SN, Hruban RH, Eby YS, Couch MJ, Forastiere AA, Sidransky D. Association between cigarette smoking and mutation of the p53 gene in squamous cell carcinoma of the head and neck. *N Engl J Med* 1995: **332**: 712–717.
13. Cabrini RL, Folco A, Savino MT, Schwint AT, Itoiz ME. A technique for section thickness evaluation for microphotometry and image analysis of sectioned nuclei. *Anal Cell Pathol* 1998: **17**: 125–130.
14. Cabrini RL, Schwint AE, Méndez A, Femopase F, Lanfranchi H, Itoiz ME. Morphometric study of nucleolar organizer regions in human oral normal mucosa, papilloma and squamous cell carcinoma. *J Oral Pathol Med* 1992: **21**: 275–279.
15. Cardoso JE, Trivillin VA, Heber EM, Nigg DW, Calzetta O, Blaumann H, Longhino J, Itoiz ME, Bumaschny E, Pozzi E, Schwint AE. Effect of Boron Neutron Capture Therapy (BNCT) on normal liver regeneration: towards a novel therapy for liver metastases. *Int J Radiat Biol* 2007: **83**: 699–706.
16. Carinci F, Pelucchi S, Farina A, Bonsetti G, Mastrandrea M, Calearo C. Site-dependent survival in cancer of the oral cavity. *J Craniofac Surg* 1997: **8**: 399–403.
17. Carmeliet P, Jain RK. Angiogenesis in cancer and other diseases. *Nature* 2000: **407**: 249–257.
18. Carnelio S, Rodrigues GS, Shenoy R, Fernández D. A brief review of common oral premalignant lesions with emphasis on their management and cancer prevention. *Indian J Surg* 2011: **73**: 256–261.
19. Chen PT, Kuan FC, Huang CE, Chen MF, Huang SH, Chen MC, Lee KD. Incidence and patterns of second primary malignancies following oral cavity cancers in a prevalent area of betel-nut chewing: a population-based cohort of 26,166 patients in Taiwan. *Jpn J Clin Oncol* 2011: **41**: 1336–1343.
20. Chen YK, Lin LM. DMBA-induced hamster buccal pouch carcinoma and VX2-induced rabbit cancer as a model for human oral carcinogenesis. *Expert Rev Anticancer Ther* 2010: **10**: 1485–1496.
21. Chu TY, Shen CY, Lee HS, Liu HS. Monoclonality and surface lesion-specific microsatellite alterations in premalignant and malignant neoplasia of uterine cervix: a local field effect of genomic instability and clonal evolution. *Genes Chromosom Cancer* 1999: **24**: 127–134.
22. Coderre JA, Morris GM. The radiation biology of boron neutron capture therapy. *Radiat Res* 1999: **151**: 1–18.
23. Coffey R, Shipley G, Moses H. Production of transforming growth factors by human colon cancer lines. *Cancer Res* 1986: **46**: 1164–1169.
24. Copper MP, Braakhuis BJ, de Vries N, van Dongen GA, Nauta JJ, Snow GBA. Panel of biomarkers of carcinogenesis of the upper aerodigestive tract as potential intermediate endpoints in chemoprevention trials. *Cancer (Phila.)* 1993: **71**: 825–830.
25. Coutts JC, Gallagher JT. Receptors for fibroblast growth factors. *Immunol Cell Biol* 1995: **37**: 584–589.
26. Crissman JD, Visscher DW, Sarkar FH. Premalignant lesions of the upper aerodigestive tract: biomarkers of genetic alterations, proliferation and differentiation. *J Cell Biochem Suppl* 1993: **17F**: 192–198.

27. Crocker J, Nar P. Nucleolar organizer regions in lymphomas. *J Pathol* 1987: **151**: 111–118.
28. Crocker J, Skilbeck N. Nucleolar organizer region associated proteins in cutaneous melanotic lesions: a quantitative study. *J Clin Pathol* 1987: **40**: 885–889.
29. Derenzini M, Ploton D. Interphase nucleolar organizer regions in cancer cells. *Int Rev Exp Pathol* 1991: **32**: 150–164.
30. Derka S, Vairaktaris E, Papakosta V, Vassiliou S, Acil Y, Vylliotis A, Spyridonidou S, Lazaris AC, Mourouzis C, Kokkori A, Moulavasili P, Perrea D, Donta I, Yapijakis C, Patsouris E. Cell proliferation and apoptosis culminate in early stages of oral oncogenesis. *Oral Oncol* 2006: **42**: 540–550.
31. Elangovan T, Mani NJ, Malathi N. Argyrophilic nucleolar organizer regions in inflammatory, premalignant, and malignant oral lesions: a quantitative and qualitative assessment. *Indian J Dent Res* 2008: **19**: 141–146.
32. Feulgen R, Rossenbeck H. Mikroskopischemischer Nachweis einer Nucleinsäure von Typus der Thymonucleinsäure und auf die darauf beruhende elektive Farbung von Zellkernen in mikroskopischen Präparaten. *Zeitschr F Physiol Chem* 1924: **135**: 203–248.
33. Folkman J, Watson K, Ingber D, Hanahan D. Induction of angiogenesis during the transition from hyperplasia to neoplasia. *Nature* 1989: **339**: 58–61.
34. Folkman J. Incipient angiogenesis. *J Natl Cancer Inst* 2000: **92**: 94–95.
35. Forastiere AA, Goepfert H, Maor M, Pajak TF, Weber R, Morrison W, Glisson B, Trotti A, Ridge JA, Chao C, Peters G, Lee DJ, Leaf A, Ensley J, Cooper J. Concurrent chemotherapy and radiotherapy for organ preservation in advanced laryngeal cancer. *N Engl J Med* 2003: **349**: 2091–2098.
36. Forsti A, Louhelainen J, Soderberg M, Wijkstrom H, Hemminki K. Loss of heterozygosity in tumour-adjacent normal tissue of breast and bladder cancer. *Eur J Cancer* 2001: **37**: 1372–1380.
37. Franklin WA, Gazdar AF, Haney J, Wistuba II, La Rosa FG, Kennedy T, Ritchey DM, Miller YE. Widely dispersed p53 mutation in respiratory epithelium. A novel mechanism for field carcinogenesis. *J Clin Invest* 1997: **100**: 2133–2137.
38. Gabel D, Fairchild RG, Larsson B. The relative biological effectiveness in V79 Chinese hamster cells in the neutron capture reaction in boron and nitrogen. *Radiat Res* 1984: **98**: 307–316.
39. Gandolfo M, Keszler A, Lanfranchi H, Itoiz ME. Increased subepithelial vascularization and VEGF expression reveal potentially malignant changes in human oral mucosa lesions. *Oral Surg Oral Med Oral Pathol Oral Radiol Endod* 2011: **111**: 486–493.
40. Ge L, Meng W, Zhou H, Bhowmick N. Could stroma contribute to field cancerization? *Med Hypotheses* 2010: **75**: 26–31.
41. Ghadimi BM, Sackett DL, Difilippantonio MJ, Schröck E, Neumann T, Jauho A, Auer G, Ried T. Centrosome amplification and instability occurs exclusively in aneuploid, but not in diploid colorectal cancer cell lines, and correlates with chromosomal numerical aberrations. *Genes Chromosom Cancer* 2000: **27**: 183–190.
42. Givol D, Yayon A. Complexity of FGF receptors: genetic basis for structural diversity and functional specificity. *FASEB J* 1992: **6**: 3362–3369.
43. Greaves P, Filipe M, Branfoot A. Transitional mucosa and survivalin human colorectal cancer. *Cancer* 1980: **46**: 764–770.
44. Gullino PM. Angiogenesis and oncogenesis. Review. *J Natl Cancer Inst* 1978: **61**: 639–643.
45. Hagendoorn J, Tong R, Fukumura D, Lin Q, Lobo J, Padera TP, Xu L, Kucherlapati R, Jain RK. Onset of abnormal blood and lymphatic vessel function and interstitial hypertension in early stages of carcinogenesis. *Cancer Res* 2006: **66**: 3360–3364.
46. Hanahan D, Weinberg RA. Hallmarks of cancer: the next generation. *Cell* 2011: **144**: 646–674.
47. Hanahan D, Folkman J. Patterns and emerging mechanisms of the angiogenic switch during tumorigenesis. *Cell* 1996: **86**: 353–364.
48. Hashibe M, Brennan P, Benhamou S, Castellsague X, Chen C, Curado MP, Dal Maso L, Daudt AW, Fabianova E, Fernandez L, Wünsch-Filho V, Franceschi S, Hayes RB, Herrero R, Koifman S, La Vecchia C, Lazarus P, Levi F, Mates D, Matos E, Menezes A, Muscat J, Eluf-Neto J, Olshan AF, Rudnai P, Schwartz SM, Smith E, Sturgis EM, Szeszenia-Dabrowska N, Talamini R, Wei Q, Winn DM, Zaridze D, Zatonski W, Zhang ZF, Berthiller J, Boffetta P. Alcohol drinking in never users of tobacco, cigarette smoking in never drinkers, and the risk of head and neck cancer: pooled analysis in the International Head and Neck Cancer Epidemiology Consortium. *J Natl Cancer Inst* 2007: **99**: 777–789.
49. Heber E, Trivillin V, Nigg D, Kreimann EL, Itoiz ME, Rebagliati RJ, Batistoni D, Schwint AE. Biodistribution of GB-10 (Na(2)(10)B10H10) in an experimental model of oral cancer in the hamster cheek pouch. *Arch Oral Biol* 2004: **49**: 313–324.
50. Heber EM, Aromando RF, Trivillin VA, Itoiz ME, Nigg DW, Kreimann EL, Schwint AE. Therapeutic effect of boron neutron capture therapy (BNCT) on field cancerized tissue: inhibition of DNA synthesis and lag in the development of second primary tumors in precancerous tissue around treated tumors in DMBA-induced carcinogenesis in the hamster cheek pouch oral cancer model. *Arch Oral Biol* 2007: **52**: 273–279.
51. Heber EM, Kueffer PJ, Lee MW Jr, Hawthorne MF, Garabalino MA, Molinari AJ, Nigg DW, Bauer W, Monti Hughes A, Pozzi EC, Trivillin VA, Schwint AE. Boron delivery with liposomes for boron neutron capture therapy (BNCT): biodistribution studies in an experimental model of oral cancer demonstrating therapeutic potential. *Radiat Environ Biophys* 2012: **51**: 195–204.
52. Heber EM, Monti Hughes A, Pozzi EC, Itoiz ME, Aromando RF, Molinari AJ, Garabalino MA, Nigg DW, Trivillin VA, Schwint AE. Development of a model of tissue with potentially malignant disorders (PMD) in the hamster cheek pouch to explore the long-term potential therapeutic and/or toxic effects of different therapeutic modalities. *Arch Oral Biol* 2010: **55**: 46–51.
53. Heber EM, Trivillin VA, Nigg DW, Itoiz ME, González BN, Rebagliati RJ, Batistoni D, Kreimann EL, Schwint AE. Homogeneous boron targeting of heterogeneous tumors for boron neutron capture therapy (BNCT): chemical analyses in the hamster cheek pouch oral cancer model. *Arch Oral Biol* 2006: **51**: 922–929.
54. Hoebers F, Heemsbergen W, Moor S, Lopez M, Klop M, Tesselaar M, Rasch C. Reirradiation for head-and-neck

cancer: delicate balance between effectiveness and toxicity. *Int J Radiat Oncol Biol Phys* 2011: **81**: e111–e118.
55. Hollows P, Mc Andrew PG, Pierini MG. Delays in the referral and treatment of oral squamous cell carcinoma. *Br Dent J* 2000: **188**: 262–265.
56. Howat A, Giri D, Cotton D, Slater D. Nucleolar organizer regions in Spitz nevi and malignant melanomas. *Cancer* 1989: **63**: 474–478.
57. Humayun S, Ram Prasad V. Expression of p53 protein and ki-67 antigen in oral premalignant lesions and oral squamous cell carcinomas: an immunohistochemical study. *Natl J Maxillofac Surg* 2011: **2**: 38–46.
58. Jan-Mohamed M, Armstrong J, Crocker J, Leyland J, Hulten M. The relationship between number of interphase NORs and NOR-bearing chromosomes in non-Hodgkin's lymphoma. *J Pathol* 1989: **158**: 3–7.
59. Janot F, el Naggar AK, Morrison RS, Liu TJ, Taylor DL, Clayman GL. Expression of basic fibroblast growth factor in squamous cell carcinoma of the head and neck is associated with degree of histologic differentiation. *Int J Cancer* 1995: **64**: 117–123.
60. Jemal A, Clegg LX, Ward E, Ries LA, Wu X, Jamison PM, Wingo PA, Howe HL, Anderson RN, Edwards BK. Annual report to the nation on the status of cancer, 1975–2001, with a special feature regarding survival. *Cancer* 2004: **101**: 3–27.
61. Jothy S, Slesak B, Harlozinska A, Lapinska J, Adamiak J, Rabczynski J. Field effect of human colon carcinoma on normal mucosa: relevance of carcinoembryonic antigen expression. *Tumour Biol* 1996: **17**: 58–64.
62. Kankaanranta L, Seppälä T, Koivunoro H, Saarilahti K, Atula T, Collan J, Salli E, Kortesniemi M, Uusi-Simola J, Mäkitie A, Seppänen M, Minn H, Kotiluoto P, Auterinen I, Savolainen S, Kouri M, Joensuu H. Boron neutron capture therapy in the treatment of locally recurred head and neck cancer. *Int J Radiat Oncol Biol Phys* 2007: **69**: 475–482.
63. Kankaanranta L, Seppälä T, Koivunoro H, Saarilahti K, Atula T, Collan J, Salli E, Kortesniemi M, Uusi-Simola J, Välimäki P, Mäkitie A, Seppänen M, Minn H, Revitzer H, Kouri M, Kotiluoto P, Seren T, Auterinen I, Savolainen S, Joensuu H. Boron neutron capture therapy in the treatment of locally recurred head-and-neck cancer: final analysis of a phase I/II trial. *Int J Radiat Oncol Biol Phys* 2012: **82**: e67–e75.
64. Kastenbauer E, Wollenberg B. In search of new treatment methods for head and neck carcinoma. *Laryngol Rhinol Otol* 1999: **78**: 31–35.
65. Kato I, Ono K, Sakurai Y, Ohmae M, Maruhashi A, Imahori Y, Kirihata M, Nazakawa M, Yura Y. Effectiveness of BNCT for recurrent head and neck malignancies. *Appl Radiat Isot* 2004: **61**: 1069–1073.
66. Klagsbrun M, Baird A. A dual receptor system is required for basic fibroblast growth factor activity. *Cell* 1991: **67**: 229–231.
67. Kreimann EL, Itoiz ME, Dagrosa A, Garavaglia R, Farías S, Batistoni D, Schwint AE. The hamster cheek pouch model of oral cancer for boron neutron capture therapy studies: selective delivery of boron by boronophenylalanine. *Cancer Res* 2001: **61**: 8775–8781.
68. Kreimann EL, Itoiz ME, Longhino J, Blaumann H, Calzetta O, Schwint AE. Boron neutron capture therapy for the treatment of oral cancer in the hamster cheek pouch model. *Cancer Res* 2001: **61**: 8638–8642.
69. Lawson M, White L, Coyle P, Butler R, Roberts-Thomson I, Conyers A. An assessment of proliferative and enzyme activity in transitional mucosa adjacent to colonic cancer. *Cancer* 1989: **64**: 1061–1066.
70. Leong AS-Y, Gilham P. Silver staining of nucleolar organizer regions in malignant melanoma and melanotic nevi. *Hum Pathol* 1989: **20**: 257–262.
71. Letchoumy PV, Chandra Mohan KV, Kumaraguruparan R, Hara Y, Nagini S. Black tea polyphenols protect against 7,12-dimethylbenz[a]anthracene-induced hamster buccal pouch carcinogenesis. *Oncol Res* 2006: **16**: 167–178.
72. Lopes NN, Plapler H, Chavantes MC, Lalla RV, Yoshimura EM, Alves MT. Cyclooxygenase-2 and vascular endothelial growth factor expression in 5-fluorouracil-induced oral mucositis in hamsters: evaluation of two low-intensity laser protocols. *Support Care Cancer* 2009: **17**: 1409–1415.
73. Luna MA, Pineda-Daboin K. Upper aerodigestive tract. In: Henson D, Albores Saavedra J, editors. *Pathology of incipient neoplasia*. New York: Oxford University Press, 2001: 57–85.
74. Lundgren C, Auer G, Frankendal B, Moberger B, Nilsson B, Nordström B. Nuclear DNA content, proliferative activity, and p53 expression related to clinical and histopathologic features in endometrial carcinoma. *Int J Gynecol Cancer* 2002: **12**: 110–118.
75. Luzi P, Bruni A, Mangiavacchi P, Cevenini G, Marini D, Tosi P. Ploidy pattern and cell cycle in breast cancer as detected by image analysis flow cytometry. *Cytometry* 1994: **18**: 79–87.
76. Mehrotra R, Gupta A, Singh M, Ibrahim R. Application of cytology and molecular biology in diagnosing premalignant or malignant oral lesions. *Mol Cancer* 2006: **5**: 11–19.
77. Molinari AJ, Aromando RF, Itoiz ME, Garabalino MA, Monti Hughes A, Heber EM, Pozzi EC, Nigg DW, Trivillin VA, Schwint AE. Blood vessel normalization in the hamster oral cancer model for experimental cancer therapy studies. *Anticancer Res* 2012: **32**: 2703–2709.
78. Molinari AJ, Pozzi EC, Monti Hughes A, Heber EM, Garabalino MA, Thorp SI, Miller M, Itoiz ME, Aromando RF, Nigg DW, Trivillin VA, Schwint AE. Tumor blood vessel "normalization" improves the therapeutic efficacy of boron neutron capture therapy (BNCT) in experimental oral cancer. *Radiat Res* 2012: **177**: 59–68.
79. Molinari AJ, Pozzi ECC, Monti Hughes A, Heber EM, Garabalino MA, Thorp SI, Miller M, Itoiz ME, Aromando RF, Nigg DW, Quintana J, Santa Cruz GA, Trivillin VA, Schwint AE. "Sequential'' Boron Neutron Capture Therapy (BNCT): a novel approach to BNCT for the treatment of oral cancer in the hamster cheek pouch model. *Radiat Res* 2011: **175**: 463–472.
80. Monti Hughes A, Heber EM, Pozzi E, Nigg DW, Calzetta O, Blaumann H, Longhino J, Nievas SI, Aromando RF, Itoiz ME, Trivillin VA, Schwint AE. Boron neutron capture therapy (BNCT) inhibits tumor development from precancerous tissue: an experimental study that supports a potential new application of BNCT. *Appl Radiat Isot* 2009: **67**(Suppl): S313–S317.
81. Monti Hughes A, Pozzi ECC, Heber EM, Thorp S, Miller M, Itoiz ME, Aromando RF, Molinari AJ, Garabalino MA, Nigg

DW, Trivillin VA, Schwint AE. Boron Neutron Capture Therapy (BNCT) in an oral precancer model: therapeutic benefits and potential toxicity of a double application of BNCT with a six-week interval. *Oral Oncol* 2011: **47**: 1017–1022.
82. Monti Hughes A, Pozzi ECC, Thorp S, Garabalino MA, Farías RO, González SJ, Heber EM, Itoiz ME, Aromando RF, Molinari AJ, Miller M, Nigg DW, Curotto P, Trivillin VA, Schwint AE. Boron Neutron Capture Therapy for oral pre-cancer: proof of principle in an experimental animal model. *Oral Diseases* 2013: **19**: 789–795.
83. Morelatto RA, Herrera MC, Fernández EN, Corball AG, López de Blanc SA. Diagnostic delay of oral squamous cell carcinoma in two diagnosis centres in Córdoba, Argentina. *J Oral Pathol Med* 2007: **36**: 405–408.
84. Morelatto RA, López de Blanc SA. Oral cancer mortality in the province of Cordoba, Argentine Republic in the period 1975–2000. A comparative study with other populations. *Med Oral Patol Oral Cir Bucal* 2006: **11**: E230–E235.
85. Morris L. Factors influencing experimental carcinogenesis in the hamster cheek pouch. *J Dent Res* 1961: **40**: 3–15.
86. Morris LG, Sikora AG, Hayes RB, Patel SG, Ganly I. Anatomic sites at elevated risk of second primary cancer after an index head and neck cancer. *Cancer Causes Control* 2011: **22**: 671–679.
87. Nagabhushan M, Line D, Polverini PJ, Solt DB. Anticarcinogenic action of diallyl sulfide in hamster buccal pouch and forestomach. *Cancer Lett* 1992: **66**: 207–216.
88. Nagini S, Letchoumy PV, Thangavelu A, Ramachandran CR. Of humans and hamsters: a comparative evaluation of carcinogen activation, DNA damage, cell proliferation, apoptosis, invasion, and angiogenesis in oral cancer patients and hamster buccal pouch carcinomas. *Oral Oncol* 2009: **45**: e31–e37.
89. Nagini S. Of humans and hamsters: the hamster buccal pouch carcinogenesis model as a paradigm for oral oncogenesis and chemoprevention. *Anticancer Agents Med Chem* 2009: **9**: 843–852.
90. Napier SS, Speight PM. Natural history of potentially malignant oral lesions and conditions: an overview of the literature. *J Oral Pathol Med* 2008: **37**: 1–10.
91. Orrea S, Tomasi VH, Schwint A, Itoiz M. Modifications to the silver staining technique for nucleolar organizer regions to improve the accuracy of image analysis. *Biotech Histochem* 2001: **76**: 67–73.
92. Padera TP, Stoll BR, Tooredman JB, Capen D, di Tomaso E, Jain RK. Pathology: cancer cells compress intratumour vessels. *Nature* 2004: **427**: 695.
93. Parkin DM, Bray F, Ferlay J, Pisani P. Global cancer statistics, 2002. *CA Cancer J Clin* 2005: **55**: 74–108.
94. Pérez MA, Raimondi AR, Itoiz ME. An experimental model to demonstrate the carcinogenic action of oral chronic traumatic ulcer. *J Oral Pathol Med* 2005: **34**: 17–22.
95. Perkins TM, Shklar G. Delay in hamster buccal pouch carcinogenesis by aspirin and indomethacin. *Oral Surg Oral Med Oral Pathol* 1982: **53**: 170–178.
96. Pindborg JJ, Murti PR, Bhonsle RB, Gupta PC, Daftary DK, Mehta FS. Oral submucous fibrosis as a precancerous condition. *Scand J Dent Res* 1984: **92**: 224–229.
97. Pindborg JJ. Oral submucous fibrosis: a review. *Ann Acad Med Singapore* 1989: **18**: 603–607.
98. Ploton D, Menager M, Jeanneson P, Himber G, Pigeon F, Adnet JJ. Improvement in the staining and in the visualization of the argyrophylic proteins of the nucleolar organizer region at the optical level. *Histochem J* 1986: **18**: 5–14.
99. Pozzi E, Migg DW, Miller M, Thorp SI, Heber EM, Zarza L, Estryk G, Monti Hughes A, Molinari AJ, Garabalino M, Itoiz ME, Aromando RF, Quintana J, Trivillin VA, Schwint AE. Dosimetry and radiobiology at the new RA-3 Reactor Boron Neutron Capture Therapy (BNCT) facility: application to the treatment of experimental oral cancer. *Appl Radiat Isot* 2009: **67**: S309–S312.
100. Prevo LJ, Sanchez CA, Galipeau PC, Reid BJ. p53-mutant clones and field effects in Barrett's esophagus. *Cancer Res* 1999: **59**: 4784–4787.
101. Raimondi A, Cabrini R, Itoiz ME. Ploidy analysis of field cancerization and cancer development in the hamster cheek pouch carcinogenesis model. *J Oral Pathol Med* 2005: **34**: 227–231.
102. Raimondi AR, Molinolo AA, Itoiz ME. Fibroblast growth factor-2 expression during experimental oral carcinogenesis. Its possible role in the induction of pre-malignant fibrosis. *J Oral Pathol Med* 2006: **35**: 212–217.
103. Rajput D, Tupkari J. Early detection of oral cancer: PAP and AgNOR staining in brush biopsies. *J Oral Maxillofac Pathol* 2010: **14**: 52–58.
104. Rosenthal AN, Ryan A, Hopster D, Jacobs IJ. Molecular evidence of a common clonal origin and subsequent divergent clonal evolution in vulvul intraepithelial neoplasia, vulval squamous cell carcinoma and lymph node metastases. *Int J Cancer* 2002: **99**: 549–554.
105. Russo A, Bazan V, Migliavacca M, Tubiolo C, Macaluso M, Zanna I, Corsale S, Latteri F, Valerio MR, Pantuso G, Morello V, Dardanoni G, Latteri MA, Colucci G, Tomasino RM, Gebbia N. DNA aneuploidy and high proliferative activity but not K-ras-2 mutations as independent predictors of clinical outcome in operable gastric carcinoma. *Cancer* 2001: **92**: 294–302.
106. Saito T, Notani K, Miura H, Fukuda H, Mizuno S, Shindoh M, Amemiya A. DNA analysis of oral leukoplakia by flow cytometry. *Int J Oral Maxillofac Surg* 1991: **20**: 259–263.
107. Saito T, Yamashita T, Notani K, Fukuda H, Mizuno S, Shindoh M, Amemiya A. Flow cytometric analysis of nuclear DNA content in oral leukoplakia: relation to clinicopathologic findings. *Int J Oral Maxillofac Surg* 1995: **24**: 44–47.
108. Salley JJ. Experimental carcinogenesis in the cheek pouch of the Syrian hamster. *J Dent Res* 1954: **33**: 253–262.
109. Sarode SC, Sarode GS, Tupkari JV. Oral potentially malignant disorders: precising the definition. *Oral Oncol* 2012: **48**: 759–760.
110. Schimming R, Hlawitschka M, Haroske G, Eckelt U. Prognostic relevance of DNA image cytometry in oral cavity carcinomas. *Anal Quant Cytol Histol* 1998: **20**: 43–51.
111. Schwint AE, Folco A, Morales A, Cabrini RL, Itoiz ME. AgNOR mark epithelial foci in malignant transformation in hamster cheek pouch carcinogenesis. *J Oral Pathol Med* 1996: **25**: 20–24.
112. Schwint AE, Gomez E, Itoiz ME, Cabrini RL. Nucleolar organizer regions as markers of incipient cellular alterations in squamous epithelium. *J Dent Res* 1993: **72**: 1233–1236.

113. Schwint AE, Savino TM, Lanfranchi HE, Marschoff E, Cabrini RL, Itoiz ME. Nucleolar organizer regions in lining epithelium adjacent to squamous cell carcinoma of human oral mucosa. *Cancer* 1994: **73**: 2674–2679.
114. Shklar G, Eisenberg E, Flynn E. Immunoenhancing agents and experimental leukoplakia and carcinoma of the buccal pouch. *Prog Exp Tumor Res* 1979: **24**: 269–282.
115. Slaga TJ, Gimenez-Conti IB. An animal model for oral cancer. Review. *J Natl Cancer Inst Monogr* 1992: **13**: 55–60.
116. Slaughter D, Southwick H, Smejkal W. "Field cancerization" in oral stratified squamous epithelium: clinical implications of multicentric origin. *Cancer* 1953: **6**: 963–968.
117. Sonis ST. A biological approach to mucositis. *J Support Oncol* 2004: **2**: 21–32. discussion 35–36.
118. Sonis ST. Mucositis: the impact, biology and therapeutic opportunities of oral mucositis. *Oral Oncol* 2009: **45**: 1015–1020.
119. Srinivasan M, Jewell SD. Evaluation of TGF-alpha and EGFR expression in oral leukoplakia and oral submucous fibrosis by quantitative immunohistochemistry. *Oncology* 2001: **61**: 284–292.
120. Srinivasan M, Jewell SD. Quantitative estimation of PCNA, c-myc, EGFR and TGF-alpha in oral submucous fibrosis – an immunohistochemical study. *Oral Oncol* 2001: **37**: 461–467.
121. Stern RS, Bolshakov S, Nataraj AJ, Ananthaswamy HN. p53 mutation in non melanoma skin cancers occurring in psoralen ultraviolet a-treated patients: evidence for heterogeneity and field cancerization. *J Invest Dermatol* 2002: **119**: 522–526.
122. Sudbø J, Kildal W, Risberg B, Koppang HS, Danielsen HE, Reith A. DNA content as a prognostic marker in patients with oral leukoplakia. *N Engl J Med* 2001: **344**: 1270–1278.
123. Sudbø J, Ried T, Bryne M, Kildal W, Danielsen H, Reith A. Abnormal DNA content predicts the occurrence of carcinomas in non-dysplastic oral white patches. *Oral Oncol* 2001: **37**: 558–565.
124. Tabor M, Brakenhoff H, van Houten VM, Kummer JA, Snel MH, Snijders PJ, Snow GB, Leemans CR, Braakhuis BJ. Persistence of genetically altered fields in head and neck cancer patients: biological and clinical implications. *Clin Cancer Res* 2001: **7**: 1523–1532.
125. Tabor MP, Brakenhoff RH, Ruijter-Schippers HJ, Kummer A, Leemans R, Braakhuis BJM. Genetically altered fields as origin of locally recurrent head and neck cancer. *Clin Cancer Res* 2004: **10**: 3607–3613.
126. Tonar Z, Egger GF, Witter K, Wolfesberger B. Quantification of microvessels in canine lymph nodes. *Microsc Res Tech* 2008: **71**: 760–772.
127. Trivillin VA, Heber EM, Itoiz ME, Nigg D, Calzetta O, Blaumann H, Longhino J, Schwint AE. Radiobiology of BNCT mediated by GB-10 and GB-10 + BPA in experimental oral cancer. *Appl Radiat Isot* 2004: **61**: 939–945.
128. Trivillin VA, Heber EM, Nigg DW, Itoiz ME, Calzetta O, Blaumann H, Longhino J, Schwint AE. Therapeutic success of Boron Neutron Capture Therapy (BNCT) mediated by a chemically non-selective boron agent in an experimental model of oral cancer: a new paradigm in BNCT radiobiology. *Radiat Res* 2006: **166**: 387–396.
129. Tytor M, Olofsson J, Ledin T, Brunk U, Klintenberg C. Squamous cell carcinoma of the oral cavity. A review of 176 cases with application of malignancy grading and DNA measurements. *Clin Otolaringol* 1990: **15**: 235–351.
130. Vairaktaris E, Spyridonidou S, Papakosta V, Vylliotis A, Lazaris A, Perrea D, Yapijakis C, Patsouris E. The hamster model of sequential oral oncogenesis. Review. *Oral Oncol* 2008: **44**: 315–324.
131. Van der Waal I, Scully C. Potentially malignant disorders of the oral and oropharyngeal mucosa. *Oral Oncol* 2010: **46**: 485–570.
132. Wachtler F, Hopman AHN, Wiegant J, Schwarzacher G. On the position of nucleolar organizer regions (NORs) in interphase nuclei: studies with a new, non autoradiographic *in situ* hybridization method. *Exp Cell Res* 1986: **167**: 227–240.
133. Wakulich C, Jackson-Boeters L, Daley TD, Wysocki GP. Immunohistochemical localization of growth factors fibroblast growth factor-1 and fibroblast growth factor-2 and receptors fibroblast growth factor receptor-2 and fibroblast growth factor receptor-3 in normal oral epithelium, epithelial dysplasias, and squamous cell carcinoma. *Oral Surg Oral Med Oral Pathol Oral Radiol Endod* 2002: **93**: 573–579.
134. Warnakulasuriya S, Johnson NW, van der Waal I. Nomenclature and classification of potentially malignant disorders of the oral mucosa. *J Oral Pathol Med* 2007: **36**: 575–580.
135. Warnakulasuriya S, Sutherland G, Scully C. Tobacco, oral cancer, and treatment of dependence. *Oral Oncol* 2005: **41**: 244–260.
136. Wünsch-Filho V, Camargo EA. The burden of mouth cancer in Latin America and the Caribbean: epidemiologic issues. *Semin Oncol* 2001: **28**: 158–168.
137. Yoshitake Y, Nishikawa K. Distribution of fibroblast growth factors in cultured tumor cells and their transplants. *In Vitro Cell Dev Biol* 1992: **28A**: 419–428.